

## Intrinsic electrical properties of $\text{LuFe}_2\text{O}_4$

Sara Lafuerza,<sup>1</sup> Joaquín García,<sup>1,\*</sup> Gloria Subías,<sup>1</sup> Javier Blasco,<sup>1</sup> Kazimierz Conder,<sup>2</sup> and Ekaterina Pomjakushina<sup>2</sup>

<sup>1</sup>*Instituto de Ciencia de Materiales de Aragón (ICMA), CSIC-Universidad de Zaragoza, Departamento de Física de la Materia Condensada, Pedro Cerbuna 12, 50009 Zaragoza, Spain*

<sup>2</sup>*Laboratory for Development and Methods, Paul Scherrer Institut, 5232 Villigen PSI, Switzerland*  
(Received 14 March 2013; revised manuscript received 19 August 2013; published 30 August 2013)

We here revisit the electrical properties of  $\text{LuFe}_2\text{O}_4$ , compound candidate for exhibiting multiferroicity. Measurements of dc electrical resistivity as a function of temperature, electric-field polarization measurements at low temperatures with and without magnetic field, and complex impedance as a function of both frequency and temperature were carried out in a  $\text{LuFe}_2\text{O}_4$  single crystal, perpendicular and parallel to the hexagonal  $c$  axis, and in several ceramic polycrystalline samples. Resistivity measurements reveal that this material is a highly anisotropic semiconductor, being about two orders of magnitude more resistive along the  $c$  axis. The temperature dependence of the resistivity indicates a change in the conduction mechanism at  $T_{\text{CO}} \approx 320$  K from thermal activation above  $T_{\text{CO}}$  to variable range hopping below  $T_{\text{CO}}$ . The resistivity values at room temperature are relatively small and are below  $5000 \Omega \text{ cm}$  for all samples but we carried out polarization measurements at sufficiently low temperatures, showing that electric-field polarization curves are a straight line as expected for a paraelectric or antiferroelectric material. Furthermore, no differences are found in the polarization curves when a magnetic field is applied either parallel or perpendicular to the electric field. The analysis of the complex impedance data corroborates that the claimed colossal dielectric constant is a spurious effect mainly derived from the capacitance of the electrical contacts. Therefore, our data unequivocally evidence that  $\text{LuFe}_2\text{O}_4$  is not ferroelectric.

DOI: [10.1103/PhysRevB.88.085130](https://doi.org/10.1103/PhysRevB.88.085130)

PACS number(s): 71.30.+h, 77.22.Ej, 77.22.Ch, 72.80.Sk

### I. INTRODUCTION

The possibility of simultaneous control of the magnetic and electronic degrees of freedom is a subject of intense interest.<sup>1</sup> Some multiferroic materials have been identified as showing coexistence and strong interplay between two *a priori* unrelated phenomena: ferroelectricity and magnetism.<sup>1,2</sup> Ferroelectricity driven by either magnetic or charge ordering has been claimed at the origin of materials phenomenology with large coupling between both properties.<sup>3</sup>

Among the multiferroics,  $\text{LuFe}_2\text{O}_4$  is considered as a prototype material where ferroelectricity is driven by the electronic process of frustrated ( $\text{Fe}^{2+}/\text{Fe}^{3+}$ ) charge ordering (CO) at  $T_{\text{CO}} \approx 320$  K, which is also coupled to magnetism and magnetic field.<sup>4–7</sup>  $\text{LuFe}_2\text{O}_4$  belongs to the rare-earth-iron oxide family  $R\text{Fe}_2\text{O}_4$  ( $R = \text{Ho-Lu}$  and  $\text{Y}$ ) adopting a layered structure.<sup>8</sup> It is a mixed valence oxide since the formal iron valence is 2.5. Above 320 K, it has a rhombohedral crystal structure (space group  $R\bar{3}m$ ) that can be described as an alternating stacking of  $[\text{LuO}_2]_\infty$  layers and  $[\text{Fe}_2\text{O}_4]_\infty$  bilayers along the hexagonal  $c$  axis. The separation of  $[\text{Fe}_2\text{O}_4]_\infty$  bilayers by the  $[\text{LuO}_2]_\infty$  layers leads to a pseudobidimensional (2D) structure for the Fe-O sublattice.<sup>9</sup>  $\text{LuFe}_2\text{O}_4$  undergoes successive phase transitions. 2D charge correlations are observed below 500 K, while the ferroelectric phase transition is proposed to coincide with a 3D  $\text{Fe}^{3+}/\text{Fe}^{2+}$  CO below 320 K.<sup>4,5,10</sup> This is followed by ferrimagnetic order below  $T_{\text{N}} \sim 240$  K.<sup>2,11–13</sup>

The general claim about ferroelectricity in  $\text{LuFe}_2\text{O}_4$  has been based on the following experimental results: (i) the observation of giant dielectric constant at temperatures above 150 K,<sup>4–6</sup> and (ii) the measurement of the pyroelectric current after field polarization.<sup>4,5,14</sup> The colossal dielectric properties reported for  $\text{LuFe}_2\text{O}_4$  (Refs. 4–6) were accepted as originating

from the motion of the ferroelectric domain boundary due to electron exchange between  $\text{Fe}^{2+}$  and  $\text{Fe}^{3+}$ . However, it has been lately pointed out that the large dielectric permittivity values may be misleading due to extrinsic effects related to its relative high electrical conductivity and the charge-depleted interface at the electrode contact or grain boundaries,<sup>15–17</sup> suggesting that the electronic ferroelectric order in  $\text{LuFe}_2\text{O}_4$  below 320 K has to be questioned. A definite proof to check for ferroelectric order is measuring the electric-field-dependent polarization [ $P(E)$ ]. Until now, banana-like  $P(E)$  loops have been reported in polycrystalline samples at about 120 K and low frequencies<sup>18,19</sup> that were interpreted as ferroelectric hysteresis curves. Nevertheless such loops are nothing but artefacts resulting from the relative high conductivity of  $\text{LuFe}_2\text{O}_4$  at these temperatures.<sup>20</sup> Indeed, the apparent ferroelectric remanent polarization values for  $\text{LuFe}_2\text{O}_4$  at about 120 K coming out from the mentioned works, that is, 0.25 (Ref. 18) and 0.05 (Ref. 19)  $\mu\text{C cm}^{-2}$ , do not agree either between them or with the reported value of near 30  $\mu\text{C cm}^{-2}$  deduced from pyroelectric current measurements.<sup>4</sup> On the contrary, a  $P(E)$  curve obtained in another recent work for a polycrystal sample at 140 K and rather high frequency of 80 kHz (Ref. 17) shows a nearly linear response suggesting the lack of ferroelectricity. Regrettably the applied electric field of 0.2 kV/cm in the latter work is by far below the typical values of coercive fields for the ferroelectric materials [usually about tens of kV/cm (Ref. 21)]. Therefore, such electric field is too low to polarize the presumed ferroelectric sample, even more regarding that it is not a single domain sample. No definite conclusion on either the existence or absence of ferroelectricity in the  $\text{LuFe}_2\text{O}_4$  compound can be thus derived from this study. On the other hand, a very new work<sup>7</sup> reports on the occurrence of combined magnetoresistance and magnetocapacitance effects, i.e., the resistance and capacitance are suppressed by the

magnetic field, and still supports the electronic ferroelectricity of  $\text{LuFe}_2\text{O}_4$ . From the structural point of view, recent single-crystal x-ray-diffraction data agree with a structure of charged Fe nonpolar bilayers,<sup>22</sup> which is in contrast with the proposed CO with polar bilayers.<sup>4</sup> At this point, the only evidence for ferroelectricity in  $\text{LuFe}_2\text{O}_4$  is that provided by the pyroelectric current detection experiments.<sup>4</sup> However, as we will explain hereafter, there is not a possibility of reproducing such an experiment due to the high conductivity of  $\text{LuFe}_2\text{O}_4$  above the CO transition temperature.

The lack of a conclusive and thorough electrical characterization in  $\text{LuFe}_2\text{O}_4$  joined to the recently appeared controversy about its ferroelectric character motivated us to carry out a detailed study of the intrinsic electrical properties. We recall here that although the evidenced noncolossal dielectric permittivity values<sup>15–17</sup> from impedance spectroscopy point to a normal dielectric character for  $\text{LuFe}_2\text{O}_4$ , this fact does not necessarily imply a nonferroelectric character [e.g., the dielectric constant values of about 30 for the ferroelectric oxide  $\text{TbMnO}_3$  (Ref. 23)]. Above all, the conclusive proof for ferroelectricity is the measurement of a  $P(E)$  hysteretic saturated ferroelectric cycle which can only be guaranteed by applying sufficiently high electrical fields.

In this paper, we report a careful study on resistivity, electrical polarization, and impedance spectroscopy measurements to obtain the intrinsic resistance and dielectric constant of both polycrystalline and single-crystal  $\text{LuFe}_2\text{O}_4$ . Our resistivity results show the strong anisotropy of the electric transport properties along the  $c$  axis with a resistivity about two orders of magnitude higher than in the  $ab$  plane. It is also interesting that the anomaly at  $T_{\text{CO}}$  in the resistivity occurs mainly in the  $ab$  plane and the CO transition corresponds to a change in the conduction mechanism from thermal activated transport above  $T_{\text{CO}}$  to charge transport via variable range hopping below  $T_{\text{CO}}$ . We also show that the resistivity at high temperatures is low enough to prevent a proper measurement of the pyroelectric current or the  $P(E)$  curves even at temperatures as low as 120 K. Therefore, we have carried out the electrical polarization measurements at low temperatures from 10 K

up to about 100 K to avoid conductivity contributions.  $P(E)$  curves with and without an applied magnetic field do not show any spontaneous polarization. This clearly demonstrates that  $\text{LuFe}_2\text{O}_4$  is not ferroelectric and that there is not any effect of a magnetic field on the intrinsic electrical polarization. Our frequency- and temperature-dependent complex impedance data confirm the results and conclusions previously reported,<sup>15–17</sup> i.e., the giant dielectric constant is not intrinsic of the material. The relatively large electrical resistivity at temperatures near the charge ordering transition<sup>24</sup> joined to the high electrical capacity of the electrodes yield an apparent colossal dielectric constant when the electrical resistance and capacity of the contacts are not considered. Moreover, we have also checked that the use of different electrodes produces marked differences in the apparent dielectric constant. Hence, this work has allowed us to conclude that  $\text{LuFe}_2\text{O}_4$  is not a multiferroic material as it was generally believed and it puts doubts on the proposed mechanism for ferroelectricity caused by frustrated charge order.

## II. EXPERIMENT

A set of polycrystalline  $\text{LuFe}_2\text{O}_{3.95(2)}$  samples were obtained by solid state chemistry reaction from stoichiometric amounts of  $\text{Lu}_2\text{O}_3$  and  $\text{Fe}_2\text{O}_3$  and sintered at  $1200^\circ\text{C}$  in a  $\text{CO}_2/\text{CO}$  (60:40) atmosphere. Powder x-ray-diffraction (XRD) measurements confirmed that samples are single phase without noticeable impurities. The left panel of Figure 1 shows heat-capacity and magnetization measurements displaying the anomalies corresponding to the CO transition at 320 K and the ferrimagnetic transition at 240 K.

Polycrystalline  $\text{LuFe}_2\text{O}_4$  precursor for single-crystal growth was prepared by a solid-state reaction as reported in Ref. 25. Starting materials of  $\text{Lu}_2\text{O}_3$  and  $\text{Fe}_2\text{O}_3$  with 99.99% purity were mixed, pressed into pellets, and sintered at  $1200^\circ\text{C}$  during 6 h in  $\text{H}_2/\text{He}/\text{CO}_2$  atmosphere ( $\text{H}_2/\text{CO}_2$  ratio 1/3) and quenched into ice water. After grinding, the obtained powder was hydrostatically pressed in a form of rods (8 mm in diameter and 70 mm in length) and sintered at the same conditions as

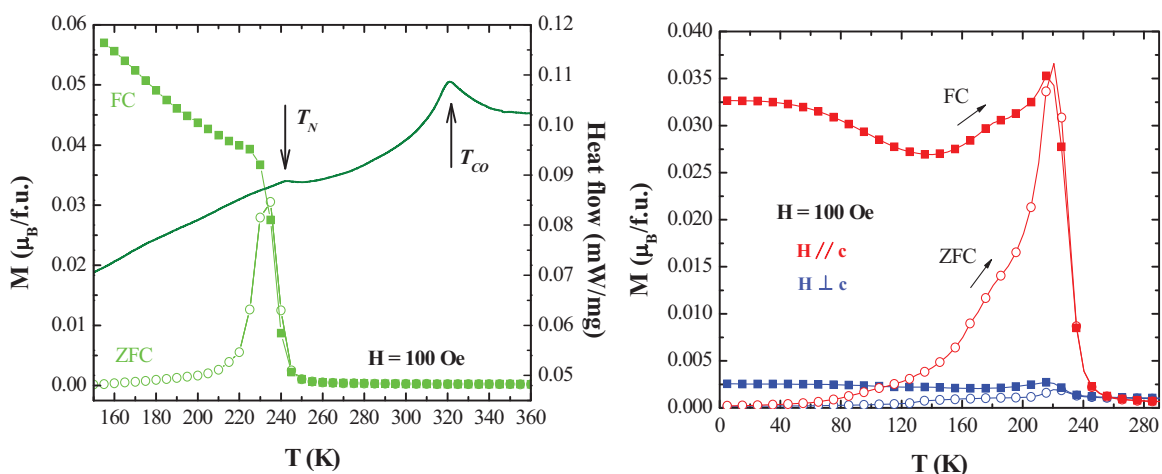


FIG. 1. (Color online) Left panel: Heat capacity and magnetization of  $\text{LuFe}_2\text{O}_4$  ceramic sample. Anomalies corresponding to the charge ordering transition at  $T_{\text{CO}} \sim 320$  K and the ferrimagnetic transition at  $T_{\text{N}} \sim 240$  K are indicated by arrows. Right panel: Temperature dependence for the magnetization of the  $\text{LuFe}_2\text{O}_4$  single crystal with the magnetic field  $\mathbf{H}$  (100 Oe) parallel (easy axis) and perpendicular (hard axis) to the hexagonal  $c$  axis. ZFC and FC in both panels stand for zero-field-cooled and field-cooled magnetization, respectively.

powder during 3 h. The crystal growth was carried out using Optical Floating Zone Furnace (FZ-T-10000-H-IV-VP-PC, Crystal System Corp., Japan) using four 1000-W halogen lamps as a heat source, growth rate 1 mm/h, 2 bars pressure of CO<sub>2</sub>/CO mixture (5/2 ratio). Phase purity was checked with x-rays using a D8 Advance Bruker AXS diffractometer with Cu  $K\alpha$  radiation. Oxygen stoichiometry was determined using thermogravimetric hydrogen reduction<sup>26</sup> and was found as 3.94(2). Two pieces were cut and polished with the surfaces perpendicular to the [001] and [110] hexagonal directions. The samples have been characterized by means of electrical, heat capacity, and magnetic measurements. The temperature dependence of the zero-field-cooled (ZFC) and field-cooled (FC) magnetization with the magnetic fields applied parallel and perpendicular to the  $c$  axis are shown in the right panel of Fig. 1. The strong magnetic anisotropy with an easy magnetic axis parallel to the  $c$  axis, the ZFC-FC magnetic irreversibility in both geometries, and the sharp magnetic transition below 240 K are in accordance with previous reports in the literature.<sup>11,27–29</sup>

Electrical dc resistivity measurements were made on sintered polycrystalline bar-shaped samples ( $\rho_{\text{pol}}$ ) with a size of  $1 \times 2 \times 6 \text{ mm}^3$  and on single-crystal bar-shaped samples of a size of  $0.5 \times 0.6 \times 1 \text{ mm}^3$  and  $0.5 \times 1 \times 4 \text{ mm}^3$  with the electric field parallel ( $\rho_c$ ) and perpendicular ( $\rho_{\text{ab}}$ ) to the hexagonal  $c$  axis. The conventional four-probe configuration was used and electrodes were made using silver paint. The electrical resistance was measured dynamically by using an Oxford N<sub>2</sub> cryostat and a furnace in cooling and heating runs at an average speed of 2 K/min. Heating and cooling runs were coincident.

Electrical polarization versus electric-field loops measurements were performed on platelike single crystals using silver paint in sandwich geometry with a typical electrode area of about 10 mm<sup>2</sup> and thickness of 0.9 mm. Disc-shaped pellets of polycrystalline samples of about 100 mm<sup>2</sup> surface and 0.8 mm thick were also measured. The sample polarization was recorded using a commercial polarization analyzer (aixACCT Systems Easy Check 300) for frequencies up to 250 Hz and electric-field amplitude of a few tens of kV/cm. It was not possible to obtain reliable  $P(E)$  hysteresis loops above 140 K due to the large leakage currents<sup>20</sup> because of the low electric resistance of LuFe<sub>2</sub>O<sub>4</sub>. Therefore, the polarization measurements were carried out down to 77 K in the Oxford N<sub>2</sub> cryostat and in a Quantum Design PPMS cryostat at temperatures below. In both cases, a homemade sample insert well electrically isolated and screened was used. The *in vacuo* signal in an open circuit configuration for both sample inserts was checked being less than 1% of the sample responses. Finally, the polarization measurements in the PPMS cryostat were also realized in the presence of a magnetic field of 60 kOe in both geometries, parallel and perpendicular to the electric field.

The dielectric measurements were carried out as a function of temperature between 77 and 300 K in a N<sub>2</sub> cryostat employing a homemade coaxial-line inset. The dielectric response was measured using an impedance analyzer (Wayne Kerr Electronics 6500B) applying voltages with amplitude of 1 V and for frequencies from 100 Hz to 1 MHz. All measurements were done in the same samples as the  $P(E)$  curves. For the sake of comparison, contacts with silver paint and soldered indium metal were prepared. We note that together with the inaccuracy

in determining the exact dimensions of the samples, additional errors due to stray capacitances imply an uncertainty in the absolute values of the dielectric constant of about 20%. Frequency dependence analysis of the impedance (real and imaginary components) was performed at selected temperatures.

### III. RESULTS

#### A. Resistivity

Figure 2 shows the temperature dependence of the electrical resistivity in oriented single crystals and ceramic polycrystalline samples. The high resistivity at low temperatures limits the temperature range of our experimental setup between 120 and 390 K. The resistivity along the hexagonal  $c$  axis,  $\rho_c$ , is two orders of magnitude higher than  $\rho_{\text{ab}}$  as expected from the strong structural anisotropy. The high  $\rho_c$  clearly indicates that the main conduction path is within the [Fe<sub>2</sub>O<sub>4</sub>]<sub>∞</sub> bilayers formed by iron atoms in a triangular lattice sharing oxygen atoms. The bilayers form a 2D lattice where electrons can move whereas the bilayers are well separated along the  $c$  axis and the electronic transfer from one bilayer to another is very difficult. Such anisotropy was also observed in the related compound YFe<sub>2</sub>O<sub>4</sub>.<sup>30</sup> As expected, the resistivity of the ceramic pellet,  $\rho_{\text{pol}}$ , has intermediate values between  $\rho_c$  and  $\rho_{\text{ab}}$ . At 290 K,  $\rho_{\text{pol}}$  is  $\sim 125 \text{ } \Omega \text{ cm}$  in agreement with previous published results,<sup>31–33</sup> whereas  $\rho_c$  is  $\sim 9 \text{ k}\Omega \text{ cm}$ . As shown in Fig. 2, the slope in the resistivity curves shows an anomaly around 320 K matching the CO transition. The slope change is more evident in the  $\rho_{\text{ab}}$  but also quite noticeable in  $\rho_{\text{pol}}$ . Although a semiconductorlike behavior is observed in the whole temperature range, we can distinguish two different transport regimes for  $T > 320 \text{ K}$  and  $T < 290 \text{ K}$ . Above  $T_{\text{CO}} \sim 320 \text{ K}$ , the data are well described with an Arrhenius law, yielding activation energies of 0.32, 0.39, and 0.24 eV for  $\rho_{\text{pol}}$ ,  $\rho_c$ , and  $\rho_{\text{ab}}$  respectively, which agree with the ones reported in Refs. 4 and 31. However, below  $T_{\text{CO}}$  the experimental data are best fitted by the law  $\rho \propto \exp(T_0/T)^{1/4}$ , expected for a variable range hopping (VRH). The inset of

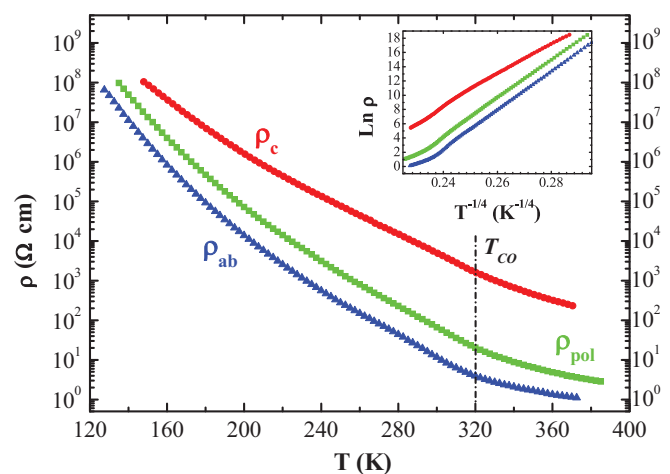


FIG. 2. (Color online) Electrical resistivity vs temperature curves for LuFe<sub>2</sub>O<sub>4</sub> single crystals parallel ( $\rho_c$ ) and perpendicular ( $\rho_{\text{ab}}$ ) to the  $c$  axis and for the polycrystalline sample ( $\rho_{\text{pol}}$ ). Inset: Plot of  $\ln \rho$  vs  $T^{-1/4}$  for the same samples.

Fig. 2 shows the plot of resistivity vs  $T^{-1/4}$ . According to Mott's VRH model<sup>34</sup> which assumes constant density of states in the vicinity of the Fermi level,  $N(E_F)$ , the characteristic temperatures  $T_0$  derived from the  $T^{-1/4}$  dependence are  $(5.08 \times 10^9)$ ,  $(2.07 \times 10^9)$ , and  $(5.29 \times 10^9)$  K for  $\rho_{\text{pol}}$ ,  $\rho_c$ , and  $\rho_{\text{ab}}$  respectively.  $T_0$  and  $N(E_F)$  are related by the equation  $T_0 = 18.1/[K_B \xi^3 N(E_F)]$  where  $\xi$  and  $K_B$  stand for localization length and Boltzmann constant, respectively. Taking a physical localization length of  $\xi = 10^{-7}$  cm, the values of  $N(E_F)$  obtained from the curves of Fig. 2 range between  $4 \times 10^{16}$  and  $1 \times 10^{17}$  eV<sup>-1</sup> cm<sup>-3</sup>. These values are typical of a band gap suggesting the hopping between distant localized states within the gap, in agreement with previous studies.<sup>31</sup> In order to test the accuracy of the VRH mechanism, we have estimated the average hopping distance ( $R$ ) and average hopping barrier ( $W$ ) from Mott's relationships:<sup>34</sup>  $R/\xi = 3/8 (T_0/T)^{1/4}$  and  $W = \frac{1}{4} K_B T (T_0/T)^{1/4}$ . At 150 K, the value of  $R$  is around 25 times the localization length whereas the hopping energy is around 0.2 eV, i.e., more than one order of magnitude higher than  $K_B T$ . Therefore, the dominant conduction mechanism in LuFe<sub>2</sub>O<sub>4</sub> changes from thermal activated charge transport above  $T_{\text{CO}}$  to a 3D VRH of noninteracting electrons below  $T_{\text{CO}}$ .

### B. Electrical polarization

Electric-field-dependent polarization measurements were performed at sufficiently low temperature in both single-crystal and polycrystalline samples to check for the occurrence of a ferroelectric hysteresis loop. In Fig. 3(a) there are some examples of the  $P(E)$  curves in the single crystal with  $E$  along the  $c$  axis at 77, 110, and 130 K. It can be observed that the  $P(E)$  dependence at 77 K is a straight line characteristic of a dielectric material. As the temperature increases, an apparent hysteresis cycle appears like those reported earlier<sup>18,19</sup> which actually reflects the increase of the sample conductivity.<sup>20</sup> The same behavior was repeated for the polycrystalline sample. Additionally, polarization measurements were carried out down to 10 K. Figure 3(b) shows the polarization curve for the highest electric field permitted by the experimental setup (of about 30 kV/cm) at 10 K for the single crystal. Again, the  $P(E)$  curve shows a linear dependence and no spontaneous polarization is detected. These results unquestionably evidence the lack of the spontaneous electrical polarization postulated to develop along the  $c$ -axis direction.<sup>4</sup> Moreover, polarization measurements for the two samples were undertaken at 10 K after cooling down from room temperature in the presence of a magnetic field of 60 kOe either parallel or perpendicular to the applied electric field. No differences were found in the electrical polarization after magnetizing the samples in any of the two geometries as can be seen in the inset of Fig. 3(b) for the single crystal cut with the surface perpendicular to the  $c$  axis. The fact that the magnetic field has no effect on the electric polarization contrasts with the magnetodielectric effect that has been generally ascribed to this material.<sup>4-7</sup> However, in systems like LuFe<sub>2</sub>O<sub>4</sub>, which are not very good insulators around the magnetic transition, magnetoresistive artifacts can also give rise to large magnetocapacitance effects.<sup>35</sup>

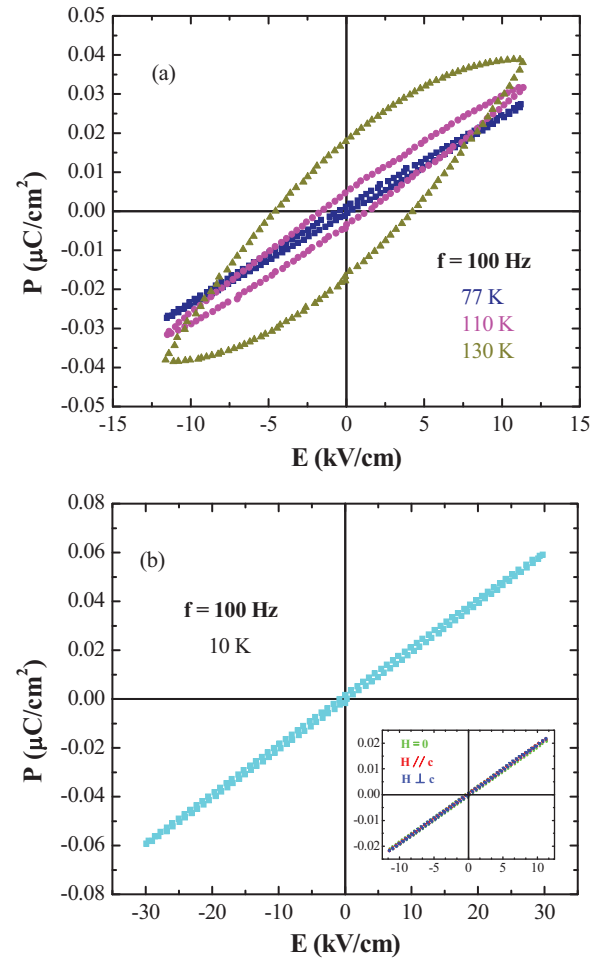


FIG. 3. (Color online) (a)  $P(E)$  curves measured on the LuFe<sub>2</sub>O<sub>4</sub> single-crystal sample with the electric field along the  $c$ -axis direction at three selected temperatures indicated in the figure for a frequency of 100 Hz. (b)  $P(E)$  curve measured on the LuFe<sub>2</sub>O<sub>4</sub> single-crystal sample with an electric field applied along the  $c$ -axis direction up to about 30 kV/cm at 10 K for a frequency of 100 Hz. Inset: Comparison of the  $P(E)$  curves measured for the same sample at 10 K and 100 Hz after zero magnetic field cooling and field cooling down from room temperature in the presence of a magnetic field  $H$  of 60 kOe applied parallel and perpendicular to  $E$ .

### C. Dielectric constant

Impedance spectroscopy was also carried out to complement the electrical polarization data at temperatures such that the sample conductivity is relevant and masks the capacitive response. Measurements with silver paint and indium metal in the same single-crystal and polycrystalline samples interpreted with only one RC (resistor and capacitor)-parallel element yielded very different values for the dielectric constant thus implying a main nonintrinsic contribution coming from the contacts (electrode/sample interface) as previously indicated.<sup>17</sup> As can be checked in Fig. 4, our samples measured with silver paint electrodes show the expected frequency dependence for relaxation processes with high-temperature and low-frequency colossal dielectric constants in agreement with other works.<sup>15-17</sup> To reveal the intrinsic features of the dielectric response, we evaluated the frequency dependence of



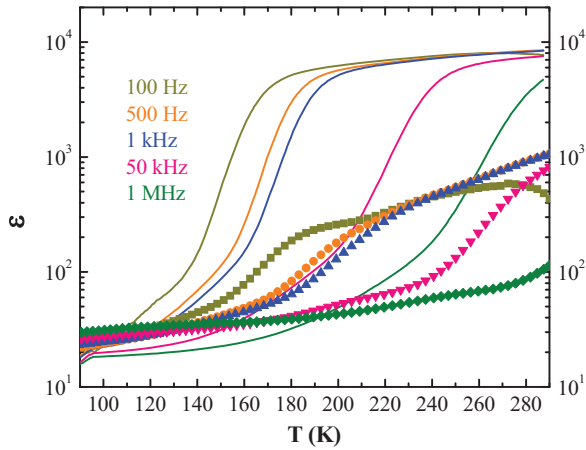


FIG. 4. (Color online) Temperature dependence of the dielectric constant of LuFe<sub>2</sub>O<sub>4</sub> polycrystalline (solid lines) and single crystal along the *c*-axis (symbols) samples measured at five frequencies using silver paint contacts deduced from a model considering only one RC-parallel element.

the complex dielectric permittivity for temperatures between 180 and 300 K. The data were quantitatively analyzed by the equivalent-circuit model generally used in impedance spectroscopy analysis. The intrinsic contribution from the LuFe<sub>2</sub>O<sub>4</sub> samples is modelled with three elements in parallel (see illustration in Fig. 5): the bulk dc resistance ( $R_S$ ), the high-frequency limit of the bulk capacitance ( $C_S$ ), and a frequency-dependent term for the ac resistance  $A\omega^{-s}$  ( $\omega = 2\pi f$ ) that accounts for the hopping conductivity contribution of the localized charge carriers according to the universal dielectric response law  $\sigma_{ac} = \sigma_0\omega^s$ .<sup>24</sup> In addition to this contribution, our equivalent-circuit model contains another parallel RC-element representing the resistance ( $R_C$ ) and capacitance ( $C_C$ ) of extrinsic contributions, mainly the electrode contacts, connected in series with the sample element. The real and imaginary components of the complex impedance  $Z'$  and  $Z''$  respectively, were fitted simultaneously as a function of frequency at various temperatures applying the model described. Figure 5 shows representative Cole-Cole plots,  $Z''$  vs  $Z'$ , with the best fitting results displayed as solid lines for both the crystal and the polycrystalline samples using electrodes with silver paint. In the case of the polycrystalline sample, the main contribution in the  $Z'$ - $Z''$  curves at 240 K arises from the contacts whereas the sample contribution comes up progressively with decreasing temperature as the small semicircle at low  $Z'$  [see Fig. 5(a)]. On the other hand, the measurements on the crystal along the *c* axis show the smallest influence from the contacts. The sample contribution can be discerned, although still tiny, at 300 K and at 260 K it is already larger than that of the contacts [see Fig. 5(b)]. The temperature dependence of the fitted parameters,  $R_S$ ,  $C_S$ ,  $R_C$ , and  $C_C$ , is shown in Fig. 6 for the polycrystalline sample (upper panel) and the single crystal (lower panel). The frequency-dependent ac resistance at a frequency of 1 MHz and the parameter  $s \approx 0.6$  (not shown) possesses a temperature dependence similar to the dc resistance  $R_S$ , increasing with decreasing temperature between 380  $\Omega$  (300 K) and 5600  $\Omega$  (180 K) for the polycrystalline sample while for the single crystal it varies from  $6 \times 10^4 \Omega$  (300 K) to  $4 \times 10^5 \Omega$  (180 K). The resistance of the electrode

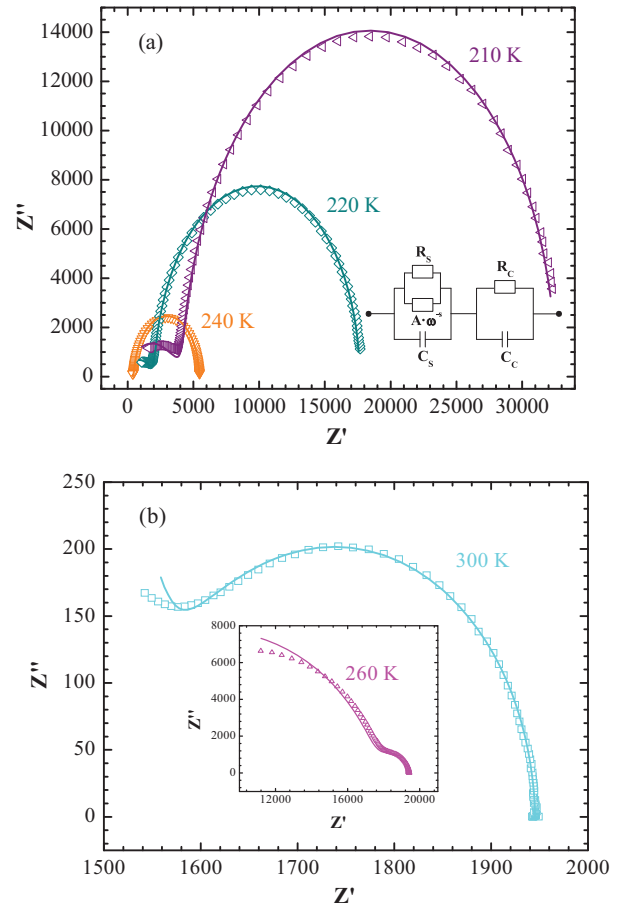


FIG. 5. (Color online) The complex impedance plots for LuFe<sub>2</sub>O<sub>4</sub> (a) polycrystalline and (b) single crystal along the *c*-axis samples at selected temperatures in linear scale. Symbols and lines are measured and fitted results, respectively. Inset of (a) shows the equivalent circuit used for fitting.

contact  $R_C$  and the bulk  $R_S$  also increase as the temperature decreases. For the polycrystalline sample, the resistance of the electrode contact is higher than the sample resistance, whereas the situation reverts for the single crystal because of the higher resistivity along *c* as already seen. The values of the contact capacitances are similar in the two cases and, regarding the sample capacitance, that of the crystal is smaller compared to the polycrystalline one according to the minor area of the first. It is to be noted that a large indeterminacy was obtained for the  $C_S$  parameter in the case of the polycrystalline sample between 300 and 240 K and for  $C_C$  in the crystal case below 220 K, indicating that the model is not sensitive to the determination of these parameters when their contribution is practically negligible.

#### IV. DISCUSSION AND CONCLUDING REMARKS

In Fig. 7 we get together our results for the intrinsic dielectric permittivity and resistivity as a function of temperature for both the polycrystalline and the single crystal (along the *c* axis) samples. On one hand can be seen the comparison of the intrinsic dielectric constant derived from the electrical polarization measurements and the complex impedance

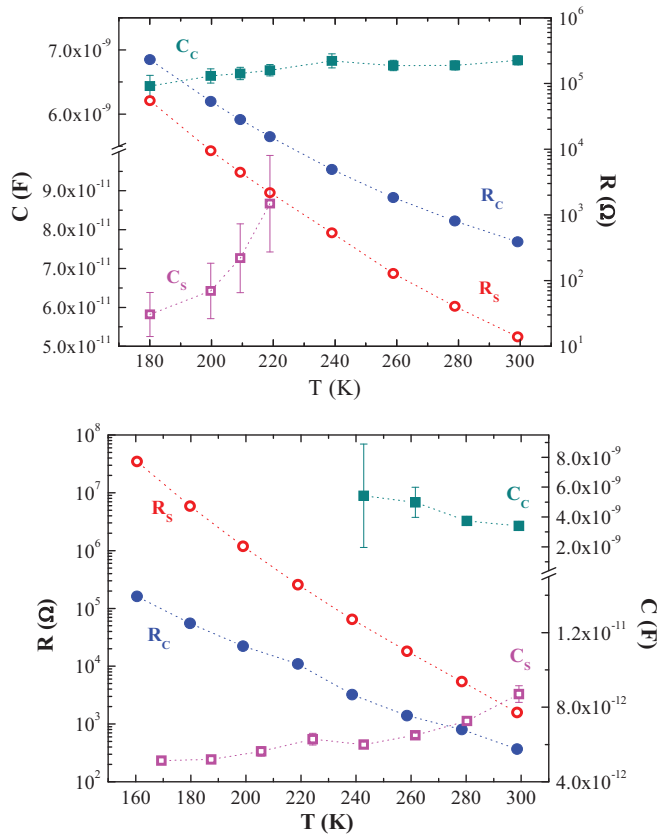


FIG. 6. (Color online) Temperature evolution of the fitted parameters  $R_s$ ,  $C_s$ ,  $R_c$ ,  $C_c$  as described in the text for LuFe<sub>2</sub>O<sub>4</sub> polycrystalline (upper panel) and single crystal (lower panel) along the  $c$ -axis direction.

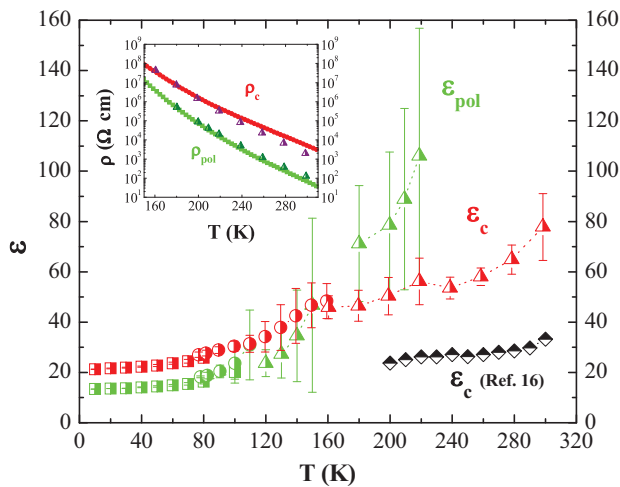


FIG. 7. (Color online) Comparison of the intrinsic dielectric constant derived from the electric-field-dependent polarization measurements (squares and circles) and the complex impedance analysis (triangles) in the LuFe<sub>2</sub>O<sub>4</sub> polycrystalline and single crystal along the  $c$  axis. Inset: For the same samples, intrinsic resistivity data derived from the analysis of the complex impedance (triangles) compared to the four-probe dc resistivity data. For the sake of comparison, intrinsic permittivity data for LuFe<sub>2</sub>O<sub>4</sub> along the  $c$  axis obtained from Ref. 16 have been included (diamonds).

analysis. The values deduced from the polarization measurements extend to temperatures such that no contribution from sample conduction was observed in the  $P(E)$  curves, being the contact capacitance values much larger than that of the sample (as can be extrapolated from Fig. 6) and therefore they can be reasonably assumed to be intrinsic. Indeed, the dielectric constant values determined from the low-temperature  $P(E)$  dependence (square and circle symbols) connect very well with those deduced from the impedance analysis at higher temperatures (triangle symbols). The intrinsic permittivity values that we have obtained are of about 10–20 at low temperatures and below 100 near room temperature. These values are high but of the same order of magnitude as those earlier reported as can be seen in Fig. 7 where we have included the intrinsic permittivity data derived by Niermann *et al.*<sup>16</sup> for LuFe<sub>2</sub>O<sub>4</sub> single crystal along the  $c$  axis (diamond symbols). On the other hand, the inset accounts for the values of the intrinsic resistivity derived from the analysis of the complex impedance compared to the four-probe dc resistivity data, showing a reasonable agreement among them and providing in this way consistency to our analysis.

To summarize, this work on the characterization of the intrinsic electrical properties of the LuFe<sub>2</sub>O<sub>4</sub> oxide allows concluding the following:

(i) As deduced from the electrical resistivity measurements, the LuFe<sub>2</sub>O<sub>4</sub> material is a highly anisotropic semiconductor, being about two orders of magnitude more resistive along the  $c$  axis. Also, it is noteworthy that the CO transition is manifested in a change of slope in the resistivity mainly in the  $ab$  plane and as variation from thermal activated transport above  $T_{CO}$  to conduction due to hopping processes below.

(ii) The apparent ferroelectric hysteresis loops in the  $P(E)$  dependence obtained for LuFe<sub>2</sub>O<sub>4</sub> actually come from the high electrical conductivity of the samples and for measurements collected at sufficient low temperatures where the electrical conductivity is small enough, no spontaneous polarization is observed. In addition, the absence of changes in the  $P(E)$  curves measured under field-cooling conditions with magnetic fields up to 60 kOe indicates the lack of correlation between magnetism and the electric polarization.

(iii) The intrinsic dielectric constant of both the single crystal (along the  $c$  axis) and polycrystalline samples seems to increase slightly with temperature from 10 to 300 K but its magnitude stays always lower than 100, the normal value also found in other transition-metal oxides. Finally, we note that the dielectric constant absolute values at high temperatures are somewhat higher for the polycrystalline sample. A contribution coming from the grain boundaries is not discarded but it should be taken into account that the conductivity for this sample was also higher implying a stronger uncertainty on the determination of epsilon as evidenced by the larger error bars.

(iv) There still remains a point of controversy concerning the reported spontaneous polarization determined by pyroelectric current measurements.<sup>4,5,14</sup> As followed from Ref. 5, the sample was polarized above  $T_{CO} \approx 320$  K with an electric field of 10 kV/cm and cooled down in the presence of this field to the liquid-nitrogen temperature. We would like to remark

that we were unable to reproduce this experiment since the application of such an electric field would imply a dissipated power of near 1000 W resulting in a strong joule heating of the sample. This opens the question about the ferroelectric state obtained from the pyroelectric effect and a further investigation about the origin of the pyroelectric current in LuFe<sub>2</sub>O<sub>4</sub> is quite necessary.

## ACKNOWLEDGMENTS

It is a pleasure to thank Dr. J. Stankiewicz for her assistance in the electrical measurements. Financial support from the Spanish MINECO (Project No. MAT2012-38213-C02-01) and Diputación General de Aragón (DGA-CAMRADS) is gratefully acknowledged. S. Lafuerza thanks DGA for the research grant.

\*jgr@unizar.es

- <sup>1</sup>S. W. Cheong and M. Mostovoy, *Nat. Mater.* **6**, 13 (2007).
- <sup>2</sup>V. Efremov, J. V. D. Brink, and D. I. Khomskii, *Nat. Mater.* **3**, 853 (2004).
- <sup>3</sup>J. van den Brink and D. I. Khomskii, *J. Phys.: Condens. Matter* **20**, 434217 (2008).
- <sup>4</sup>N. Ikeda, H. Ohsumi, K. Ohwada, K. Ishii, T. Inami, K. Kakurai, Y. Murakami, K. Yoshii, S. Mori, Y. Horibe, and H. Kito, *Nature (London)* **436**, 1136 (2005).
- <sup>5</sup>N. Ikeda, *J. Phys.: Condens. Matter* **20**, 434218 (2008).
- <sup>6</sup>M. A. Subramanian, T. He, J. Z. Chen, N. S. Rogado, T. G. Calvarese, and A. W. Sleight, *Adv. Mater.* **18**, 1737 (2006).
- <sup>7</sup>T. Kambe, Y. Fukada, J. Kano, T. Nagata, H. Okazaki, T. Yokoya, S. Wakimoto, K. Kakurai, and N. Ikeda, *Phys. Rev. Lett.* **110**, 117602 (2013).
- <sup>8</sup>N. Kimizuka, E. Muromachi, and K. Siratori, in *Handbook on the Physics and Chemistry of Rare Earths*, edited by K. A. Gschneider Jr. and L. Eyring (Elsevier Science, Amsterdam, 1990), Vol. 13, pp. 283–384.
- <sup>9</sup>M. Isobe, N. Kimizuka, J. Iida, and S. Takekawa, *Acta Crystallogr. C* **46**, 1917 (1990).
- <sup>10</sup>Y. Yamada, K. Kitsuda, S. Nohdo, and N. Ikeda, *Phys. Rev. B* **62**, 12167 (2000).
- <sup>11</sup>J. Iida, M. Tanaka, Y. Nakagawa, S. Funahashi, N. Kimizuka, and S. Takekawa, *J. Phys. Soc. Jpn.* **62**, 1723 (1993).
- <sup>12</sup>K. Yoshii, N. Ikeda, Y. Matsuo, Y. Horibe, and S. Mori, *Phys. Rev. B* **76**, 024423 (2007).
- <sup>13</sup>A. D. Christianson, M. D. Lumsden, M. Angst, Z. Yamani, W. Tian, R. Jin, E. A. Payzant, S. E. Nagler, B. C. Sales, and D. Mandrus, *Phys. Rev. Lett.* **100**, 107601 (2008).
- <sup>14</sup>R. A. Mc Kinnon, Ph.D. thesis, University of Warwick, 2011.
- <sup>15</sup>P. Ren, Z. Yang, W. G. Zhu, C. H. A. Huan, and L. Wang, *J. Appl. Phys.* **109**, 074109 (2011).
- <sup>16</sup>D. Niermann, F. Waschkowski, J. de Groot, M. Angst, and J. Hemberger, *Phys. Rev. Lett.* **109**, 016405 (2012).
- <sup>17</sup>A. Ruff, S. Krohns, F. Schrettle, V. Tsurkan, P. Lunkenheimer, and A. Loidl, *Eur. Phys. J. B* **85**, 290 (2012).
- <sup>18</sup>J. Y. Park, J. H. Park, Y. K. Jeong, and H. M. Jang, *Appl. Phys. Lett.* **91**, 152903 (2007).
- <sup>19</sup>D. S. F. Viana, R. A. M. Gotardo, L. F. Cotica, I. A. Santos, M. Olzon-Dionysio, S. D. Souza, D. Garcia, J. A. Eiras, and A. A. Coelho, *J. Appl. Phys.* **110**, 034108 (2011).
- <sup>20</sup>J. F. Scott, *J. Phys.: Condens. Matter* **20**, 021001 (2008).
- <sup>21</sup>W. Prellier, M. P. Singh, and P. Murugavel, *J. Phys.: Condens. Matter* **17**, R803 (2005).
- <sup>22</sup>J. de Groot, T. Mueller, R. A. Rosenberg, D. J. Keavney, Z. Islam, J. W. Kim, and M. Angst, *Phys. Rev. Lett.* **108**, 187601 (2012).
- <sup>23</sup>T. Kimura, T. Goto, H. Shintani, K. Ishizaka, T. Arima, and Y. Tokura, *Nature (London)* **426**, 55 (2003).
- <sup>24</sup>P. Lunkenheimer, V. Bobnar, A. V. Pronin, A. I. Ritus, A. A. Volkov, and A. Loidl, *Phys. Rev. B* **66**, 052105 (2002).
- <sup>25</sup>J. Iida, S. Takekawa, and N. Kimizuka, *J. Cryst. Growth* **102**, 398 (1990).
- <sup>26</sup>K. Conder, E. Pomjakushina, A. Soldatov, and E. Mitberg, *Mater. Res. Bull.* **40**, 257 (2005).
- <sup>27</sup>W. Wu *et al.*, *Phys. Rev. Lett.* **101**, 137203 (2008).
- <sup>28</sup>J. Kim, S. B. Kim, C. U. Jung, and B. W. Lee, *IEEE Trans. Magn.* **45**, 2608 (2009).
- <sup>29</sup>J. de Groot *et al.*, *Phys. Rev. Lett.* **108**, 037206 (2012).
- <sup>30</sup>M. Tanaka, J. Akimitsu, Y. Inada, N. Kimizuka, I. Shindo, and K. Siratori, *Solid State Commun.* **44**, 687 (1982).
- <sup>31</sup>B. Fisher, J. Genossar, L. Patiagan, and G. M. Reisner, *J. Appl. Phys.* **109**, 084111 (2011).
- <sup>32</sup>C. Li, X. Zhang, Z. Cheng, and Y. Sun, *Appl. Phys. Lett.* **93**, 152103 (2008).
- <sup>33</sup>J. Bourgeois *et al.*, *Phys. Rev. B* **85**, 064102 (2012).
- <sup>34</sup>N. F. Mott and E. A. Davis in *Electronic Processes in Non-Crystalline Materials* (Oxford University Press, Oxford, 1979).
- <sup>35</sup>G. Catalan, *Appl. Phys. Lett.* **88**, 102902 (2006).